Surface Plasmon Resonance Biosensor Studies of Human Wild-Type and Mutant Lecithin Cholesterol Acyltransferase Interactions with Lipoproteins†

Lihua Jin,‡ Jeng-Jong Shieh,§ Edith Grabbe,§ Shanthi Adimoolam,‡ Diane Durbin,‡ and Ana Jonas*,‡

Department of Biochemistry, University of Illinois at Urbana−Champaign, Urbana, Illinois 61801, and Monsanto Company, St. Louis, Missouri 63167

Received July 20, 1999; Revised Manuscript Received September 23, 1999

ABSTRACT: Binding of lecithin cholesterol acyltransferase (LCAT) to lipoprotein surfaces is a key step in the reverse cholesterol transport process, as the subsequent cholesterol esterification reaction drives the removal of cholesterol from tissues into plasma. In this study, the surface plasmon resonance method was used to investigate the binding kinetics and affinity of LCAT for lipoproteins. Reconstituted high-density lipoproteins (rHDL) containing apolipoprotein A-I or A-II, (apoA-I or apoA-II), low-density lipoproteins (LDL), and small unilamellar phosphatidylcholine vesicles, with biotin tags, were immobilized on biosensor chips containing streptavidin, and the binding kinetics of pure recombinant LCAT were examined as a function of LCAT concentration. In addition, three mutants of LCAT (T123I, N228K, and (Δ53−71) were examined in their interactions with LDL. For the wild-type LCAT, binding to all lipid surfaces had the same association rate constant, k_a, but different dissociation rate constants, k_d, that depended on the presence of apoA-I (k_d decreased) and different lipids in LDL. Furthermore, increased ionic strength of the buffer decreased k_a for the binding of LCAT to apoA-I rHDL. For the LCAT mutants, the Δ53−71 (lid-deletion mutant) exhibited no binding to LDL, while the LCAT-deficiency mutants (T123I and N228K) had nearly normal binding to LDL. In conclusion, the association of LCAT to lipoprotein surfaces is essentially independent of their composition but has a small electrostatic contribution, while dissociation of LCAT from lipoproteins is decreased due to the presence of apoA-I, suggesting protein−protein interactions. Also, the region of LCAT between residues 53 and 71 is essential for interfacial binding.

Lecithin cholesterol acyltransferase (LCAT)[1] catalyzes the transfer of the *sn*-2 fatty acid of phosphatidylcholine to the 3-OH group of cholesterol and thus converts cholesterol to cholesteryl ester. This reaction is a key step in reverse cholesterol transport, a pathway in which free cholesterol from peripheral cells is returned to the liver for catabolism (*1*). Cholesterol to cholesteryl ester conversion occurs preferentially on high-density lipoproteins (HDL), particularly nascent discoidal HDL (*2*,*3*). On apoB-containing lipoproteins such as low-density lipoprotein (LDL), LCAT shows much lower activity (*4*).

Similar to various lipases, LCAT is an interfacially activated enzyme (*5*) and has a lid region (between Cys50 and Cys74) that is thought to mediate its binding to lipoprotein substrates (*6*, *7*). Apolipoprotein A-I (apoA-I) on HDL is the main physiological activator of LCAT (*1*), and the region spanning residues 143−165 in apoA-I has been implicated in the activation of LCAT (*8*, *9*); however, it is not clear whether apoA-I interacts directly with LCAT or whether apoA-I activates the lipid substrates. To address this question, the interactions of LCAT with reconstituted HDL (rHDL) containing either apoA-I or apoA-II or variable phospholipids were previously studied in this laboratory by use of a solid-phase assay and an enzyme-inhibition assay (*10*, *11*). The enzyme-inhibition assay indicated a 5-fold difference in dissociation equilibrium constant (K_d) values for the rHDL containing apoA-I or apoA-II, whereas the solid-phase binding assay gave similar K_d values for binding to the two rHDL particles. While these results indicated that the effect of apolipoproteins is small on the binding affinity of LCAT for these particles, changes in their phospholipid composition, particularly increasing sphingomyelin or phosphatidylethanolamine contents up to 20 mol % of the rHDL phospholipid (phosphatidylcholine), had significant effects on LCAT binding. Thus, it was concluded that initial binding of LCAT to lipoproteins occurs to the lipid, and activation by apoA-I is a separate step that may or may not include direct interaction between LCAT and apoA-I.

† This work was supported by NIH Grant HL-29939 to A.J., and by a postdoctoral fellowship from the American Heart Association, Illinois Affiliate, to L.J.

* To whom correspondence should be addressed: Telephone (217) 333-0452; Fax (217) 333-8868; e-mail a-jonas@uiuc.edu.

‡ University of Illinois at Urbana−Champaign.

§ Monsanto Company.

[1] Abbreviations: LCAT, lecithin cholesterol acyltransferase (EC 2.3.1.43); HDL, high-density lipoproteins; LDL, low-density lipoproteins; apoA-I, apolipoprotein A-I; apoA-II, apolipoprotein A-II; rHDL, reconstituted high-density lipoproteins; SPR, surface plasmon resonance; apoA-I rHDL, reconstituted high-density lipoproteins containing apolipoprotein A-I; apoA-II rHDL, reconstituted high-density lipoproteins containing apolipoprotein A-II; SUV, small unilamellar vesicles; DPPC, dipalmitoylphosphatidylcholine; egg-PC, egg phosphatidylcholine; DPPE, dipalmitoylphosphatidylethanolamine; FC, unesterified (free) cholesterol; HABA, 2-(4′-hydroxyphenyl)azobenzoic acid; POPC, palmitoyloleoylphosphatidylcholine; RU, response units; CE, cholesterol ester; PL, phospholipid; K_d, dissociation equilibrium constant; k_d, dissociation rate constant; k_a, association rate constant.

10.1021/bi9916729 CCC: $18.00
Published on Web 11/05/1999

In this study, we addressed again the question of LCAT interaction with apoA-I on the surface of rHDL using a new approach, surface plasmon resonance (SPR) biosensor, to determine not only accurate K_d values but also the association and dissociation rate constants, which provide insights into the mechanism of macromolecular recognition. We also used the SPR biosensor method to extend our previous studies of the interaction of rHDL with human wild-type LCAT, two mutants associated with LCAT deficiencies (T123I and N228K) (*12*), and a lid-deletion mutant (*6*) to equilibrium and kinetic binding experiments with LDL. While LDL are only minor LCAT substrates in normal plasma, they become important contributors to cholesterol esterification in fish eye LCAT disease (T123I) (*13, 14*) or in severe HDL deficiencies (*15*). Also, failure of an LCAT mutant, such as the lid-deletion mutant, to bind to both HDL and LDL indicates a defect in the interfacial recognition of the enzyme.

EXPERIMENTAL PROCEDURES

Purification of Wild-Type LCAT and Mutants. Human recombinant LCAT, two naturally occurring LCAT mutants (T123I and N228K), and a lid-deletion mutant of LCAT (Δ53−71) were purified from stable *dhfr*$^-$ CHO cell lines overexpressing the above individual LCAT forms (*12, 16*). The purified enzyme forms were stored under N_2 at 4 °C in 10 mM Tris-HCl buffer with 5 mM EDTA, pH 7.4, at concentrations of 0.17−0.35 mg/mL and used within 10 months without loss of activity.

Preparation of Biotinylated rHDL and Small Unilamellar Vesicles. Discoidal apoA-I or apoA-II rHDL samples were prepared by the sodium cholate dialysis method (*17*, *18*) and were stored under N_2 at 4 °C in Tris salt buffer (10 mM Tris buffer, 150 mM NaCl, 0.1 mM EDTA, and 1 mM NaN_3), pH 8.0. Biotinylation of rHDL was performed during the preparation of rHDL by mixing a small amount of *N*-biotinylated dipalmitoylphosphatidylethanolamine (*N*-biotinyl-DPPE) (Avanti Polar Lipids) with the bulk egg phosphatidylcholine (egg-PC) or dipalmitoylphosphatidylcholine (DPPC) (Sigma) and free cholesterol (FC) (Sigma). Molar ratios of egg-PC (or DPPC)/*N*-biotinyl-DPPE/FC/apolipoprotein were 99/0.7/5/1 for the apoA-I rHDL preparation. An equal mass of apoA-II relative to apoA-I was used for the apoA-II rHDL preparation. Homogeneity of the preparations was assessed by scanning native gradient gels (8−25% polyacrylamide, Pharmacia PhastSystem) with the Ultroscan XL laser densitometer (LKB Bromma). Concentrations of apolipoproteins in the rHDL preparations were determined by both absorbance measurements and a modified Lowry assay (*19*).

Small unilamellar vesicles (SUV) were prepared by sonication of a dispersion of egg-PC, FC, and a small amount of *N*-biotinyl-DPPE (100:5:0.1 mol ratio) in Tris salt buffer, pH 8.0, and passage through a Sepharose CL-4B column (2.5 × 60 cm).

LDL Biotinylation. LDL was purified from a single unit of plasma as described previously (*20*) and dialyzed into a buffer containing 10 mM sodium phosphate, 150 mM NaCl, 0.1 mM EDTA, and 1 mM NaN_3, pH 7.4. Biotinylation was carried out with the EZ-Link sulfo-NHS-LC-biotinylation kit from Pierce Chemical Co., using conditions recommended by Pierce as modified from Hnatowich et al. (*21*). LDL at a concentration of 10 mg/mL was mixed with freshly made 1 mg/mL sulfo-NHS-LC-biotin in a molar ratio of 1:16 (LDL protein:sulfo-NHS-LC-biotin), and incubated on ice for 2 h. The reaction mixture was dialyzed against Tris salt buffer, pH 8.0, to remove unreacted sulfo-NHS-LC-biotin. An apparent biotinylation ratio was determined by reacting biotinylated LDL with an excess of HABA reagent [2-(4′-hydroxyphenyl)azobenzoic acid] and avidin (Pierce Chemical Co.). Tight binding of biotin (biotin-LDL) to avidin displaces avidin-bound HABA; therefore, it reduces the absorbance of the HABA−avidin complex at 500 nm. The biotinylation ratio is calculated from the absorbance change.

Enzyme Activity Assays and Kinetics. The enzymatic activities of wild-type LCAT with palmitoyloleoylphosphatidylcholine (POPC) apoA-I rHDL, POPC apoA-II rHDL, and LDL were determined with purified recombinant LCAT. LDL and rHDL were prepared and radiolabeled with [^{14}C]cholesterol as described previously (*17*, *22*). After correction for the incomplete incorporation of ^{14}C-cholesterol into the lipoproteins (*23*), the percent conversion of cholesterol to cholesteryl esters was used to calculate the acyltransferase reaction velocities with rHDL and LDL. The assay was performed at varying substrate concentrations to obtain apparent kinetic parameters. For apoA-I rHDL, final substrate concentrations of 1.4×10^{-7}−2.6×10^{-6} M apoA-I or 1.1×10^{-5}−2.1×10^{-4} M phospholipid were used, and the activity at each substrate concentration was measured in duplicate. For apoA-II rHDL and LDL, appropriate concentrations were selected to obtain measurable kinetic parameters, and the LCAT concentration was adjusted over a 50-fold range (12.8−640 ng/0.5 mL) so that conversion of FC to cholesteryl esters did not exceed 15%. Initial velocity data as a function of phospholipid concentration were fit to a hyperbolic, Michaelis−Menten curve by the KaleidaGraph 3.0.5 program (Abelbeck Software) to obtain the apparent V_{max} and K_m parameters.

Surface Plasmon Resonance Analysis. Analyses of LCAT binding to rHDL, LDL, and SUV were performed on BIAcore 2000 and 3000 surface plasmon resonance (SPR) instruments. All the binding experiments were carried out at 25 °C, a temperature at which the enzymatic reaction of LCAT is significantly reduced compared with reaction at 37 °C. Solutions of wild-type and LCAT mutants were diluted to 2 μM and were further diluted before use to a set of eight sample solutions with concentrations in the range from 0.02 to 2 μM in the running buffer (10 mM Tris buffer, 150 mM NaCl, and 5 mM EDTA, pH 7.6). Before SPR analysis, all samples were centrifuged at 7500 rpm for 15 s to eliminate trapped air. The running buffer was degassed by sonication under vacuum for 30 min each day, followed by filtration through a 0.2 μm filter.

The streptavidin (SA5) chip (BIAcore) in the flow cell consists of a gold surface to which a carboxymethylated dextran layer is bound. The dextran layer is activated with streptavidin by the manufacturer. Prior to the experiment, the streptavidin surface was first cleaned with a solution of 0.05 N NaOH/1 M NaCl three times, each of 1 min duration. Biotinylated rHDL, LDL, or SUV were then immobilized onto the surface through the biotin−streptavidin interaction by exposing the surface to biotinylated rHDL (0.2 mg/mL apoA-I or apoA-II), LDL (0.6 mg/mL apoB), or SUV (3 mg/mL lipids) solutions in running buffer, until 600−1200

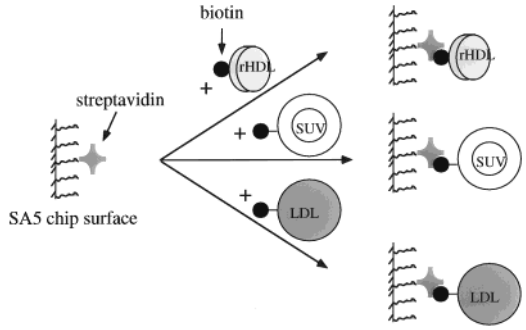

FIGURE 1: Illustration of the immobilization of biotinylated rHDL, LDL, and SUV onto a SA5 chip (streptavidin) surface. Note the accessibility of immobilized rHDL, LDL, and SUV to LCAT (about a third of rHDL mass) present in the mobile buffer phase.

response units (RU) of biotinylated rHDL, 2000−3000 RU of biotinylated LDL, or 1500−2000 RU of SUV were bound on the surface. Figure 1 illustrates the immobilization reactions for the biotinylated rHDL, LDL, and SUV. Before each experiment, the BIAcore system was cleaned to remove any residual detergents or adsorbed proteins using the "desorb" and "sanitize" procedures recommended in the BIAcore 2000 user manual.

For the experiments comparing wild-type LCAT and LCAT mutants in their binding to rHDL or LDL, two flow cells were monitored simultaneously: flow cell 1 immobilized with biotinylated DPPC/FC/apoA-I rHDL (DPPC apoA-I rHDL) and flow cell 2 immobilized with biotinylated egg-PC/FC/apoA-I rHDL (egg-PC apoA-I rHDL) in the case of rHDL binding or with biotinylated LDL in the case of LDL binding. For the experiments comparing LCAT binding to egg-PC apoA-I rHDL and egg-PC apoA-II rHDL, flow cell 3, containing immobilized egg-PC apoA-II rHDL, was also monitored at the same time. The DPPC apoA-I rHDL surface did not bind LCAT under the present experimental conditions (25 °C, 600−1200 RU of biotinylated DPPC apoA-I rHDL, and 0.02−2 μM LCAT concentrations) and was used as a control. While LCAT can bind to and react with DPPC apoA-I rHDL under favorable conditions, the binding affinity at the temperature and concentrations used in these experiments is too low (about 30-fold lower than for egg-PC apoA-I rHDL) to be observed. In the experiments where LCAT binding to immobilized SUV was examined, the control surface was the SA5 chip surface previously treated with 1 M formic acid. During each run, rHDL, LDL, or SUV surfaces were washed with running buffer for 100 s. They were then exposed to a 1 min injection of the LCAT sample solution at a flow rate of 30 μL/min. At the end of the association phase, LCAT was allowed to dissociate from the surface for 200 s by switching to the flow of the running buffer at the same flow rate. Because the catalytic rate constant for LCAT on egg-PC apoA-I rHDL is 0.05 s^{-1} at 25 °C, little or no conversion of FC to cholesteryl ester is expected to take place during the short (60 s) exposure of the immobilized particles to LCAT. LCAT dissociates quickly from rHDL and LDL surfaces, making surface regeneration with chemical reagents unnecessary. An aliquot containing only the running buffer was also injected. For the SUV surface, following the 200 s buffer wash, the surface was exposed to a 15 μL injection of a solution containing 7.5 mM Tris, 112 mM NaCl, and 4 mM EDTA, pH 9.6, which regenerated the surface.

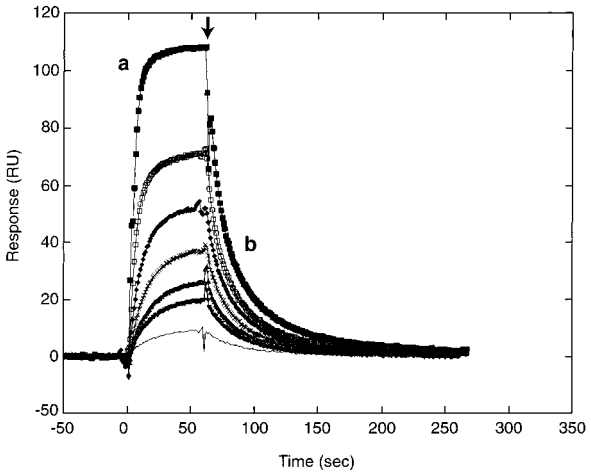

FIGURE 2: SPR sensorgrams of wild-type LCAT binding to egg-PC apoA-I rHDL at varying LCAT concentrations, obtained on a BIAcore 2000 system. Signals from a control surface (DPPC apoA-I rHDL) and from buffer runs have been subtracted. Phase **a** corresponds to the association phase (LCAT injection at 30 μL/min for 60 s); phase **b** corresponds to the dissociation phase [buffer injection (arrow) at 30 μL/min for 180 s]. From bottom to top sensorgrams, the LCAT concentrations increased from 0.02 to 0.64 μM.

Table 1: Enzymatic Activity of LCAT with Lipoprotein Particles—Apparent Kinetic Constants

lipoprotein	app V_{max}[a] (nmol of CE/hr)	app K_m (M) [PL]	app V_{max}[a]/app K_m (nmol of CE h^{-1} M^{-1})	% reactivity
POPC apoA-I rHDL[b]	11	1.03×10^{-5}	1.1×10^{6}	100
POPC apoA-II rHDL[b]	0.81	8.1×10^{-5}	1.0×10^{4}	0.91
LDL	4.8	4.9×10^{-5}	9.8×10^{4}	9.0

[a] Values of V_{max} were normalized to 1 μg of LCAT. In all cases, recombinant LCAT was used. [b] The kinetic data were obtained on POPC rHDL particles. Past experiments have indicated that POPC rHDL and egg-PC rHDL react very similarly with LCAT.

The delay in injection of LCAT or buffer into each successive flow cell was corrected in the raw data so that all flow cells had a common start time. The signal obtained from the inactive DPPC apoA-I rHDL surface or the SA5 chip surface in flow cell 1 was then subtracted from each scan for flow cells 2 and 3. The buffer scan for each flow cell was then subtracted from each LCAT scan. The sensorgrams at varying concentrations of LCAT were then fitted to a 1:1 Langmuir binding isotherm with a global fitting kinetics program supplied with the BIAcore system, from which the association rate constant, k_a (s^{-1} M^{-1}), the dissociation rate constant, k_d (s^{-1}), and the equilibrium binding constant, K_d (M, $= k_d/k_a$), were obtained. A representative set of corrected sensorgrams is shown in Figure 2.

RESULTS

Enzymatic Activity of LCAT with Lipoprotein Particles. LCAT activities with POPC apoA-I rHDL, POPC apoA-II rHDL, and native LDL were determined and the apparent kinetic constants are listed in Table 1. The apparent V_{max} values, normalized to 1 μg of wild-type LCAT, are 11, 0.81, and 4.8 nmol of CE/h for POPC apoA-I rHDL, POPC apoA-II rHDL, and LDL, respectively. Their apparent K_m values

Table 2: Kinetic and Equilibrium Binding Constants of Wild-Type LCAT Binding to ApoA-I rHDL, ApoA-II rHDL, and SUVs, Determined on BIAcore SPR Systems

surface	NaCl concn (M)	k_a (s^{-1} M^{-1})	k_d (s^{-1})	K_d (M)
apoA-I rHDL[a]	0.15	1.5×10^5 [b]	0.012	0.80×10^{-7}
	0.50	1.1×10^5	0.012	1.1×10^{-7}
	1.0	0.73×10^5	0.019	2.6×10^{-7}
apoA-II rHDL[a]	0.15	$(2.0 \pm 0.7) \times 10^5$ [b]	0.063 ± 0.012[b]	$(3.4 \pm 0.5) \times 10^{-7}$ [b]
SUV[a]	0.15	1.4×10^5	0.043	3.2×10^{-7}

[a] The reconstituted HDL particles were made with egg-PC, FC, and apolipoprotein apoA-I or apoA-II. Small unilamellar vesicles (SUV) contained egg-PC and FC. Binding experiments were carried out at 25 °C in a buffer containing 10 mM Tris, 5 mM EDTA, pH 7.6, and varying concentrations of NaCl for the apoA-I rHDL. [b] Experimental errors were of the same magnitude for all the k_a, k_d, and K_d values.

are 1.03×10^{-5}, 8.1×10^{-5}, and 4.9×10^{-5} M phospholipid, respectively. The relative reactivity [(app V_{max}/app K_m) $\times$ 100] of LCAT with the three substrates is 100% for POPC apoA-I rHDL, 0.9% for POPC apoA-II rHDL, and 9.0% for LDL.

The apparent K_m values, which reflect (to a first approximation) the affinity of LCAT for the interfacial substrates, were severalfold higher for POPC apoA-II rHDL and LDL than for POPC apoA-I rHDL, suggesting that LCAT binds more strongly to POPC apoA-I rHDL than to the other two lipoproteins, which are devoid of apoA-I. The apparent V_{max} value for POPC apoA-I rHDL was 13-fold higher than that for POPC apoA-II rHDL, consistent with the activation effect of LCAT by apoA-I on otherwise very similar particles.

LCAT Binding to Immobilized ApoA-I rHDL, ApoA-II rHDL, and SUV. Kinetics of wild-type recombinant LCAT binding to egg-PC apoA-I rHDL and egg-PC apoA-II rHDL were determined with the BIAcore 2000 surface plasmon resonance biosensor. The reconstituted lipoproteins, egg-PC apoA-I rHDL, egg-PC apoA-II rHDL, and DPPC apoA-I rHDL were prepared at the same time and biotinylated to an average of 1.4 biotins/rHDL through direct incorporation of *N*-biotinyl-DPPE into the bulk lipids during the reconstitution. The biotinylated DPPC apoA-I rHDL contained more than 98% of particles with 96 Å diameters, and the biotinylated egg-PC apoA-I rHDL or egg-PC apoA-II rHDL contained about 90% of particles with 96 or 103 Å diameters, respectively. LCAT activities with biotinylated egg-PC apoA-I rHDL in the presence and absence of streptavidin were determined to assess the effect of the tether. No significant effect of biotinylation on LCAT activity was observed in either case at the biotinylation ratio used.

Binding experiments of LCAT to the egg-PC apoA-I rHDL and egg-PC apoA-II rHDL surfaces were carried out at the same time by immobilizing egg-PC apoA-I rHDL in flow cell 2 and egg-PC apoA-II rHDL in flow cell 3 of the same streptavidin sensor chip. As no LCAT binding to DPPC apoA-I rHDL surface was observed under the conditions used, it was immobilized in flow cell 1 of the same sensor chip and used as a control surface. The signal obtained for that surface was subtracted from the signal of egg-PC apoA-I rHDL or egg-PC apoA-II rHDL surface.

During an LCAT-rHDL binding experiment, it was observed that prolonged exposure (2 min or longer) of the rHDL surface to LCAT resulted in gradual reduction of the signal (RU) that occurred before the binding reached an equilibrium. This could be due to loss of rHDL from the surface as a result of extended enzymatic reaction or destabilization of rHDL over a long period of time. The exposure time was therefore limited to only 1 min. Binding stoichiometry can often be estimated by saturating the binding sites on the immobilized macromolecule and calculating the molar ratio of the ligand macromolecule versus the immobilized one. Because of the limited exposure time, however, estimation of binding stoichiometry was not possible. A group of sensorgrams obtained at varying concentrations of LCAT for the same rHDL surface was used in curve-fitting to obtain the association (k_a) and dissociation (k_d) rate constants (see Figure 2). Values of k_a, k_d, and K_d ($=k_d/k_a$) of LCAT binding to egg-PC apoA-I rHDL and egg-PC apoA-II rHDL are given in Table 2. In the standard running buffer, which contains 150 mM NaCl, LCAT binding to egg-PC apoA-I rHDL and egg-PC apoA-II rHDL have very similar k_a values—1.5×10^5 s^{-1} M^{-1} and $(2.0 \pm 0.7) \times 10^5$ s^{-1} M^{-1}, respectively. Their k_d values, however, differ by a factor of 5—0.012 s^{-1} for apoA-I rHDL and 0.063 ± 0.012 s^{-1} for egg-PC apoA-II rHDL. Binding of LCAT to egg-PC apoA-II rHDL is weaker than to egg-PC apoA-I rHDL, as indicated by their equilibrium binding constants (K_d), $(3.4 \pm 0.5) \times 10^{-7}$ M for egg-PC apoA-II rHDL and 0.8×10^{-7} M for egg-PC apoA-I rHDL. The 4-fold difference in K_d is mainly the result of the difference in their dissociation rate constants.

In a separate experiment, performed on a BIAcore 3000 system, we examined the binding of LCAT to a SUV surface containing the same lipid proportions (egg-PC and FC) as the apoA-I rHDL and apoA-II rHDL but devoid of apolipoproteins. The results summarized in Table 2 indicate that the association rate constant, k_a, is the same for LCAT binding to SUVs (1.4×10^5 s^{-1} M^{-1}) as for LCAT binding to both rHDL. However, the k_d for LCAT dissociation from SUV is much closer to its k_d for apoA-II rHDL. Thus, the kinetics and equilibrium constant, K_d, are essentially the same for LCAT binding to apoA-II rHDL and SUV lipid surfaces.

Ionic Strength Effects on the Binding of LCAT to Egg-PC ApoA-I rHDL. The effect of salt (NaCl) concentration on LCAT binding to egg-PC apoA-I rHDL was also examined. Additional kinetic and equilibrium binding constants in running buffer containing 0.50 and 1.0 M NaCl are listed in Table 2. The dissociation rate constant (k_d) is unchanged over the range of salt concentration from 0.15 to 1.0 M. On the other hand, the association rate constant decreases with increasing salt concentration from 1.5×10^5 s^{-1} M^{-1} at 0.15 M NaCl to 1.1×10^5 s^{-1} M^{-1} at 0.5 M NaCl, to 0.73×10^5 s^{-1} M^{-1} at 1.0 M NaCl. The equilibrium binding constants, therefore, increase from 0.80×10^{-7} M at 0.15 M NaCl to 1.1×10^{-7} M at 0.5 M NaCl to 2.6×10^{-7} M at 1.0 M NaCl.

Table 3: Kinetic and Equilibrium Binding Constants of Wild-Type LCAT and LCAT Mutants Binding to LDL, Determined on a BIAcore SPR System

LCAT	k_a (s^{-1} M^{-1})	k_d (s^{-1})	K_d (M)
wild type	$(2.1 \pm 0.1) \times 10^5$	0.21 ± 0.20	$(9.9 \pm 0.5) \times 10^{-7}$
T123I[a]	$(5.5 \pm 1.5) \times 10^5$	0.37 ± 0.1	$(7.0 \pm 1.9) \times 10^{-7}$
N228K[a,b]			
lid-deletion[c]			

[a] The LCAT mutants were prepared as in ref *13*. The binding experiments were performed at 25 °C in 10 mM Tris, 150 mM NaCl, and 5 mM EDTA, pH 7.6. [b] Binding was observed, but fitting was not ideal. K_d was estimated to be higher than 1×10^{-6} M. [c] Isolated from CHO cells permanently overexpressing the lid-deletion LCAT mutant (*6*; Adimoolam et al., 1998, unpublished results). No binding was observed.

Binding of Wild-Type LCAT and LCAT Mutants to LDL. Fresh LDL purified from human plasma was biotinylated through amine coupling of sulfo-NHS-LC-biotin to apoB on LDL. The apparent biotinylation ratio was determined to be 0.59:1 (biotin:LDL) by reacting biotinylated LDL to the avidin bound HABA reagent [2-(4′-hydroxyphenyl)azobenzoic acid]. The effect of biotinylation of LDL on LCAT activity was not determined. However, at this low biotinylation ratio, the presence of biotin is unlikely to have a significant effect on LCAT activity with LDL as was the case with rHDL. Biotinylated LDL was immobilized in flow cell 2 of the SA5 sensor chip surface. DPPC apoA-I rHDL was immobilized in flow cell 1 of the same chip surface as a control. Binding kinetics of wild-type LCAT, two naturally occurring recombinant LCAT mutants (T123I and N228K), and the lid-deletion mutant (Δ53−71) to the LDL surface were determined on the BIAcore 2000 system. The resulting kinetic and equilibrium binding constants are listed in Table 3.

The association rate constant, k_a, for the binding of wild-type LCAT to LDL was $(2.1 \pm 0.1) \times 10^5$ s^{-1} M^{-1}, similar to that of apoA-I rHDL binding which was 1.5×10^5 s^{-1} M^{-1}, while the dissociation rate constant was 0.21 ± 0.20 s^{-1}, 18 times faster than for apoA-I rHDL binding. The equilibrium binding constant for LDL was $(9.9 \pm 0.5) \times 10^{-7}$ M and the binding affinity was 12-fold weaker than binding to egg-PC apoA-I rHDL (0.80×10^{-7} M). Thus, the difference in affinity is mainly due to the difference in dissociation rate constant k_d.

For the T123I LCAT mutant, the association rate constant was $(5.5 \pm 1.5) \times 10^5$ s^{-1} M^{-1}, about 3 times faster than for wild-type, and the dissociation rate constant was 0.37 ± 0.1 s^{-1}, about 2 times faster than for wild-type. Thus, the final equilibrium dissociation constant K_d was $(7.0 \pm 1.9) \times 10^{-7}$ M, close to that of wild-type LCAT binding to LDL; evidently, the T123I mutant has a similar affinity for LDL as wild type. Binding of the N228K LCAT mutant to LDL was observed, but the curve fitting was poor. The K_d was estimated to be larger than 1×10^{-6} M. No binding of the lid-deletion mutant was detected to LDL nor to egg-PC apoA-I rHDL.

DISCUSSION

Kinetics of wild-type and mutant human recombinant LCAT binding to rHDL and LDL were determined on BIAcore 2000 and 3000 systems, biosensors based on the surface plasmon resonance phenomenon. For successful determination of kinetic binding constants by this technique, the immobilized macromolecule should retain its functional interaction with the mobile ligand. Optimal immobilization chemistry is that which immobilizes macromolecules with the least steric restriction and the least reduction in accessibility for binding. In this work, the most commonly used immobilization chemistry, amine coupling on the carboxymethylated dextran surface (CM5 chip), was initially used to immobilize rHDL. However, no binding of wild-type LCAT was observed to this surface. As amine coupling of proteins to CM5 chips can involve multiple sites on each protein, the absence of binding was attributed to steric restriction of rHDL and reduced accessibility of LCAT. It is also possible that some lysine residues of apoA-I in rHDL may be required for LCAT binding but were not available after amine coupling.

Biotin−streptavidin interaction as a coupling chemistry, on the other hand, can be controlled to introduce a minimal number of coupling sites on each immobilized molecule by limiting the biotinylation ratio to close to 1 biotin molecule/macromolecule. When rHDL was biotinylated to an average ratio of 1.4 biotins/rHDL and immobilized onto a streptavidin-containing chip, LCAT binding was indeed observed and kinetic binding constants were obtained. Similarly, LDL was biotinylated to a ratio of only 0.5 biotin/LDL at which the majority of LDL molecules either have one or no biotin. One biotin attachment site per LDL should minimize the restriction of LDL dynamics at the surface. Biotinylation of SUVs was, on average, 2 biotins exposed to the external solvent per vesicle. Therefore, we believe that the kinetic and equilibrium binding constants obtained in this study are as close to the solution values as can be attained by this method.

The major advantage of using the BIAcore SPR method to measure macromolecular interactions over other methods that only provide binding equilibrium constants is the capability of observing, in real time, the kinetics of association (on rates) and dissociation (off rates) of the macromolecules. Kinetic rate constants obtained by this method provide useful information about biological specificity, not available from equilibrium measurements alone. For example, it has been shown that two monoclonal antibodies for the same macromolecular antigen may have the same equilibrium binding constant but quite different kinetic association and dissociation rate constants, reflecting differences in molecular recognition (*24*). In situations where macromolecular interactions have different equilibrium constants, knowledge of the kinetic rate constants can provide information on factors that regulate either the association or dissociation rates of the reaction. A study of mutations in the F_vCDR3 regions of an antibody to lysozyme showed that various amino acid substitutions in this antibody region did not affect its association rate constant with lysozyme but did change the dissociation rate constant (k_d) over 3 orders of magnitude (*25*). Thus, k_d is apparently very sensitive to the exact nature of the interacting amino acid side chains and reflects the disruption of short-range contacts and forces (*25*). This interpretation of the significance of k_d is applicable to most macromolecular interactions; however, the physical meaning of k_a is less apparent.

The association rate constant is a second-order rate constant that could be viewed in terms of the collision theory of chemical reactions or, alternatively, in terms of the transition-state theory (*26*). According to the collision theory, the rate constant involves terms with molecular mass of the reactants, their relative velocity, and effective cross-sectional area. On the other hand, in the transition-state theory the association rate constant is determined by the activation energy for the formation of a transient intermediate. The activation energy is determined by several energy factors including energy spent on conformational changes (*27*), decreased dynamic motion (*28*), breaking of solvent bonds and making of new bonds (such as H-bonds, van der Waals interactions, electrostatic interactions, and hydrophobic interactions) (*29*, *30*), and overcoming steric hindrance (*31*).

We conducted a limited survey of published values for k_as, obtained by the BIAcore SPR method for a variety of macromolecular interactions, and noted that they span values from 1.5×10^3 to 3.9×10^6 s^{-1} M^{-1}. Most of the results are for protein−protein interactions (k_as from 2×10^4 to 3.9×10^6 s^{-1} M^{-1}), some for protein-DNA interactions (1.5×10^3 to 10^5 s^{-1} M^{-1}), and for protein−lipid surface interactions (2×10^5 to 7×10^5 s^{-1} M^{-1}). While the sample is too limited for definitive conclusions regarding the physical basis for k_a values, the molecular weight of the mobile ligand (usually protein) appears to affect k_a, and the chemical nature of the immobilized reactant (protein, nucleic acid, or lipid particle) also seems to have a large effect. Information on solution conditions, especially ionic strength, is lacking.

In this study we examined the interaction of LCAT with egg-PC rHDL, containing either apoA-I or apoA-II. From the results of the enzymatic reaction with LCAT, we confirmed that apoA-II rHDL is only 1% as reactive as apoA-I rHDL (Table 1). This difference in reactivity could be due to a failure of the enzyme to bind to the apoA-II particles or to an inability of these particles to activate LCAT. Our results are clear in this respect—apoA-II rHDL does bind LCAT with good affinity (equilibrium constant, K_d, 3.4×10^{-7} M), but the K_d is 4-fold higher than for apoA-I rHDL. This difference agrees with our previous measurements from a solution phase assay based on the inhibition of LCAT activity by added rHDL particles (*10*). In addition, the present results include the rate constants for association and dissociation of LCAT with the immobilized rHDL (Table 2). The association constants are, within error, identical, suggesting that LCAT recognizes the same surface features of the two rHDL upon initial binding. This observation suggests that, initially, LCAT recognizes the lipid phase of rHDL (*10*, *11*). In contrast, the dissociation rate constant for LCAT from apoA-II rHDL is about 5-fold faster than from apoA-I rHDL, suggesting additional short-range interactions in the latter particles that do not exist in the apoA-II rHDL. In fact, the experiment on the binding of LCAT to SUVs provides strong support for this view: both k_a and k_d are essentially the same for SUV and for apoA-II−rHDL binding of LCAT. This implies that the association phase to the lipid is equivalent on these surfaces, and there are no further interactions (as with apoA-I) to affect the k_d. Thus, from the equilibrium constants one may calculate the standard free energy constants for the binding of LCAT in the presence and absence of apoA-I on the rHDL surface. The difference between the two $\Delta G°$ values gives a $\Delta\Delta G°$ of −0.86 kcal/mol that can be attributed to the presence of apoA-I in the rHDL and may correspond to the activation process possibly involving conformational changes in LCAT and/or apoA-I.

Previous work from this laboratory revealed that LCAT activity with rHDL varies as a function of NaCl concentration (*32*). When POPC apoA-I rHDL were used, the initial reaction rate, v_0, increased 48% from 0 to 0.1 M NaCl; however, v_0 decreased by 38% from 0.15 to 0.5 M NaCl and by 64% from 0.15 to 1.0 M NaCl. The present kinetic study showed that the affinity ($K_a = 1/K_d$) of LCAT binding to egg-PC (major component is POPC) apoA-I rHDL decreased by 38% from 0.15 to 0.5 M NaCl and by 70% from 0.15 to 1.0 M. Therefore, the effect of NaCl concentration on the affinity of LCAT binding to the rHDL surface, although small, could explain the previously seen effect of NaCl on the initial reaction rate of LCAT.

Binding of LCAT to the rHDL surface was not observed when the running buffer contained no NaCl. This was likely due to charge repulsion of the negatively charged LCAT and the negative charges of the carboxymethyl groups on the chip surface. Therefore, it was not possible to determine whether the increase in v_0 from 0 to 0.10 M NaCl observed previously was due to an increase in LCAT affinity for the rHDL surface. The effect of NaCl concentration on the binding of LCAT for rHDL comes mainly from differences in k_a values. In view of the conclusion reached earlier that apoA-I does not contribute to k_a, it follows that the salt effect on LCAT binding to rHDL is exerted on the LCAT−lipid interaction. Thus, there is a weak electrostatic contribution in the binding of LCAT to rHDL due to charges on the lipid surface.

In addition to the interactions of LCAT with rHDL discussed above, we also examined wild-type LCAT and three of its previously characterized mutants (*12*, *13*) in their binding affinity and kinetics with LDL. The initial surface recognition by LCAT is apparently nonspecific, as LDL and rHDL lipid compositions are distinct, yet their k_as are equal (see Table 3). This agrees with the report that choleratoxin binds to phosphatidylcholine vesicles containing different glycolipids with equal k_as, and only k_ds are affected (*33*). Therefore, the effects of sphingomyelin, previously observed on the binding affinity (K_d^{-1}) of LCAT for rHDL (*11*), most likely were exerted on the dissociation phase of the reaction (k_d). Similarly, the sphingomyelin in LDL may affect the dissociation of the enzyme from this lipoprotein class. Whether or not the activating effects of apoA-I are replaced in LDL by interaction of LCAT with apoB-100 cannot be determined from these results. However, even if such an interaction does occur, it clearly does not lead to the level of activation of LCAT observed with apoA-I because the enzymatic reactivity of LCAT with LDL is only 9% of that measured with apoA-I rHDL (Table 1).

The results for the binding of LCAT mutants to LDL indicate that both the T123I (fish eye disease) and N228K (familial LCAT deficiency) mutants bind to LDL with an affinity similar to that observed with wild-type LCAT. Similarly, in work we reported previously (*12*), the LCAT mutants bound to egg-PC apoA-I rHDL with K_ds comparable to that of wild-type LCAT. Thus, the defects in these mutants are not in the initial, interfacial binding step to lipoproteins but rather in subsequent steps of the reaction cycle. For the T123I (fish eye) mutant the defect is likely in the activation of the enzyme by apoA-I, and for the N228K (familial LCAT

deficiency) mutant the defect is probably in the binding of phosphatidylcholine to the active site of the enzyme, as discussed in ref *12*. In contrast to the near normal binding of the point mutants to lipoproteins, deletion of residues K53−G71 in the lid region of LCAT (*6*) completely abolishes binding of LCAT to LDL and rHDL. Thus, most likely, the lid region of LCAT is directly involved in binding to lipoprotein interfaces.

In conclusion, the surface plasmon resonance approach used to study the interaction of LCAT and immobilized lipoproteins and SUVs has provided valuable new information about factors that determine the affinity and molecular recognition: the existence of a critical lipid-binding domain in LCAT (the lid region), an association phase of interaction with lipoproteins that possibly involves some global electrostatic effects on the lipid surface but does not sense the precise liquid-crystalline lipid composition of the rHDL, LDL, and SUVs, and a dissociation phase that is sensitive to short-range interactions that likely involve apoA-I and specific classes of surface lipids.

REFERENCES

1. Fielding, C. J., and Fielding, P. E. (1995) *J. Lipid Res. 36*, 211−228.
2. Glomset, J. (1972) in *Blood Lipids and Lipoproteins* (Nelson, G., Ed.) pp 745−787, Wiley, New York.
3. Jonas, A. (1991) *Biochim. Biophys. Acta 1084*, 205−220.
4. Barter, P. J., Hopkins, G. J., and Gorjatschko, L. (1985) *Atherosclerosis 58*, 97−107.
5. Jonas, A. (1998) *Prog. Lipid Res. 37*, 209−234.
6. Adimoolam, S., and Jonas, A. (1997) *Biochem. Biophys. Res. Commun. 232*, 783−787.
7. Peelman, F., Vanloo, B., Perez-Mendez, O., Decout, A., Verschelde, J. L., Labeur, C., Vinaimont, N., Verhee, A., Duverger, N., Brasseur, R., Vandekerckhove, J., Tavernier, J., and Rosseneu, M. (1999) *Protein Eng. 12*, 71−78.
8. Minnich, A., Collet, X., Roghani, A., Cladaras, C., Hamilton, R. L., Fielding, C. J., and Zannis, V. I. (1992) *J. Biol. Chem. 267*, 16553−16560.
9. Sorci-Thomas, M., Kearns, M. W., and Lee, J. P. (1993) *J. Biol. Chem. 268*, 21403-21409.
10. Bolin, D. J., and Jonas, A. (1994) *J. Biol. Chem. 269*, 7429−7434.
11. Bolin, D. J., and Jonas, A. (1996) *J. Biol. Chem. 271*, 19152−19158.
12. Adimoolam, S., Jin, L., Grabbe, E., Shieh, J. J., and Jonas, A. (1998) *J. Biol. Chem. 273*, 32561−32567.
13. Funke, H., von Eckardstein, A., Pritchard, P. H., Albers, J. J., Kastelein, J. J. P., Droste, C., and Assmann, G. (1991) *Proc. Natl. Acad. Sci. U.S.A. 88*, 4855−4859.
14. Kuivenhoven, J. A., Pritchard, H., Hill, J., Frohlich, J., Assmann, G., and Kastelein, J. (1997) *J. Lipid Res. 38*, 191−205.
15. Schaefer, E. J., Ordovas, J. M., Law, S. W., Ghiselli, G., Kashyap, M. L., Srivastava, L. S., Heaton, W. H., Albers, J. J., Connor, W. E., Lindgren, F. T., Lemeshev, Y., Segrest, J. P., and Brewer, H. B., Jr. (1985) *J. Lipid Res. 26*, 1089−1101.
16. Jin, L., Lee, Y.-P., and Jonas, A. (1997) *J. Lipid Res. 38*, 1085−1093.
17. Matz, C., and Jonas, A. (1982) *J. Biol. Chem. 257*, 4535−4540.
18. Jonas, A. (1986) *Methods Enzymol. 128*, 553−582.
19. Markwell, M., Haas, S., Bieber, L., and Tolbert, N. (1978) *Anal. Biochem. 87*, 206−211.
20. Schumaker, V. N., and Puppione, D. L. (1986) *Methods Enzymol. 128*, 155−170.
21. Hnatowich, D. J., Virzi, F., and Rusckowski, M. (1987) *J. Nucl. Med. 28*, 1294−1302.
22. Stokke, K. T., and Norum, K. R. (1971) *Scand. J. Clin. Lab. Invest. 27*, 21−27.
23. Kosek-Burkybile, A., Durbin, D., and Jonas, A. (1999) *Biochem. Biophys. Res. Commun. 258*, 548−551.
24. Karlsson, R., Michaelsson, A., and Mattsson, L. (1991) *J. Immunol. Methods 145*, 229−240.
25. England, P., Bregegere, F., and Bedouelle, H. (1997) *Biochemistry 36*, 164−172.
26. Moore, J. W., and Pearson, R. G. (1981) in *Kinetics and Mechanism* (3rd Ed.), pp 28−38, John Wiley and Sons, New York.
27. Braden, B. C., Dall'Acqua, W., Eisenstein, E., Fields, B. A., Goldbaum, F. A., Malchiodi, E. L., Mariuzza, R. A., Schwarz, F. P., Ysern, X., and Poljak, R. J. (1995) *Pharm. Acta Helv. 69*, 225−230.
28. Carver, T. E., and Olson, J. S. (1991) *Biochemistry 30*, 4697−4705.
29. Puri, K. D., Khan, M. I., Gupta, D., and Surolia, A. (1993) *J. Biol. Chem. 268*, 16378−16387.
30. Hargrove, M. S., Barrick, D., and Olson, J. S. (1996) *Biochemistry 35*, 11293−11299.
31. Tanious, F. A., Jenkins, T. C., Neidle, S., and Wilson, W. D. (1992) *Biochemistry 31*, 11632−11640.
32. Jonas, A., Daehler, J. L., and Wilson, E. R. (1986) *Biochim. Biophys. Acta 876*, 474−485.
33. MacKenzie, C. R., Hirama, T., Lee, K. K., Altman, E., and Young, N. M. (1997) *J. Biol. Chem. 272*, 5533−5538.

BI9916729